The effect of initial discharge conditions on the properties of microcrystalline silicon thin films and solar cells*

Chen Yong-Sheng(陈永生)[a)b)], Yang Shi-E(杨仕娥)[a)], Wang Jian-Hua(汪建华)[b)c)], Lu Jing-Xiao(卢景霄)[a)], Gao Xiao-Yong(郜小勇)[a)], and Gu Jin-Hua(谷锦华)[a)†]

[a)] *Key Laboratory of Material Physics, Department of Physics, Zhengzhou University, Zhengzhou* 450052, *China*
[b)] *Institute of Plasma Physics, Chinese Academy of Sciences, Hefei* 230031, *China*
[c)] *Department of Materials Science and Engineering, Wuhan Institute of Technology, Wuhan* 430073, *China*

(Received 13 December 2008; revised manuscript received 3 November 2009)

This paper studies the effects of silane back diffusion in the initial plasma ignition stage on the properties of microcrystalline silicon (μc-Si:H) films by Raman spectroscopy and spectroscopic ellipsometry, through delaying the injection of SiH_4 gas to the reactor before plasma ignition. Compared with standard discharge condition, delayed SiH_4 gas condition could prevent the back diffusion of SiH_4 from the reactor to the deposition region effectively, which induced the formation of a thick amorphous incubation layer in the interface between bulk film and glass substrate. Applying this method, it obtains the improvement of spectral response in the middle and long wavelength region by combining this method with solar cell fabrication. Finally, results are explained by modifying zero-order analytical model, and a good agreement is found between the model and experiments concerning the optimum delayed injection time.

Keywords: back diffusion, microcrystalline silicon, thin film, Raman crystallinity
PACC: 7280N, 7830G, 8115H

1. Introduction

Plasma deposition is a key process in the fabrication of highly efficient microcrystalline silicon (μc-Si:H) thin-film solar cells. During vapour-phase deposition processing, the precise control of the initial processing stage is extremely important, due to the connection with the interface formation and nucleation,[1−7] the transient depletion of the SiH_4 source gas during roughly the first minutes of processing and the back diffusion of SiH_4 in the reactor which induced the formation of an additional incubation layer, and developed a zero-order analytical model[8] to calculate the optimum SiH_4 injection time. However, in this model, several pivotal parameters, such as the electron density and the effective dissociation rate must be known, and a mass of calculation is needed. So, this model is not applied conventionally in practice, especially for use in industrialization equipment. In this paper, the effect of SiH_4 back diffusion on the film crystallinity, microstructure, and the properties of solar cells are investigated under high pressure depletion with very high frequency (VHF) plasma processing and the results are analysed by using the modified zero-order analytical model.

2. Experimental details

Intrinsic μc-Si:H films were deposited on 15×15 cm^2 quartz glass substrates in an ultra-high vacuum deposition chamber,[9] designed as one of the process chambers of a cluster tool system. The material was grown by VHF plasma enhanced chemical vapour deposition (PECVD) at frequency 75 MHz. The size of the radio frequency (RF) electrode was 700 cm^2, and the electrode distance is fixed at 15 mm. The substrate temperature was always kept at 220 °C, total gas flow ($[SiH_4] + [H_2]$) $Q = 250$ sccm and the chamber pressure at 300 Pa. Several series of samples were deposited under delayed and standard plasma ignition conditions in SiH_4 and H_2 gas mixtures under silane concentrations (SC) (defined as $SiH_4/(SiH_4 + H_2)$) of 2% and 4%. The VHF power maintained 100 W and the deposition times changed between 1–2 min.

Raman spectroscopy (514 nm) and spectroscopic

*Project supported by the State Key Development Program for Basic Research of China (Grant No. 2006CB202601).
†Corresponding author. E-mail: chysh2003@zzu.edu.cn
© 2010 Chinese Physical Society and IOP Publishing Ltd

ellipsometry (SE) are basic non-destructive optical tools routinely employed to study the microstructural properties of μc-Si:H films. Whereas Raman data provide an average weighted by the intensity of the laser vs depth, ellipsometry is able to provide information on crystallinity vs film thickness.[2] The SE spectra of the real, $< \varepsilon_1 >$, and imaginary, $< \varepsilon_2 >$, parts of the pseudo-dielectric function, $< \varepsilon >=< \varepsilon_1 > +\mathrm{i} < \varepsilon_2 >$, were acquired with a phase modulated spectroscopic ellipsometer (Wvase32) in the range 1.5–4.0 eV with an energy step of 0.02 eV and at an angle of incidence of 70°. The SE spectra were analysed by using the Bruggeman effective medium approximation assuming the μc-Si:H films consisting of microcrystalline and amorphous silicon phases and voids. Figure 1 depicts a three-layer optical model used in the analysis of bulk film growth on glass substrate. In this model, the films consist of the following three parts: 1) the incubation amorphous interface-layer; 2) the middle bulk layer; 3) the 'growth-front' and top surface layer.

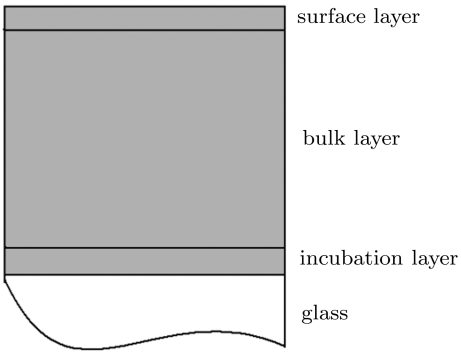


Fig. 1. The optical model used in the analysis of thin film growth.

The SnO_2/ZnO coated glass was used as substrate for single junction μc-Si:H thin film solar cells. The back contact was Al prepared by evaporation for p–i–n solar cells, and defined cell area was 0.25 cm^2. Quantum efficiency measurement is carried out with no optical bias for single-junction cells.

3. Results and discussion

3.1. Film deposition

During the μc-Si:H film deposition process, H_2 gas background, firstly, is formed inside the reactor, and then followed with SiH_4 gas after the pressure reaching stabilization. However, in order to realize the reproducibility of material properties, morphology and structures, plasma ignition takes place after SiH_4 concentration and its partial pressure reaching stabilization. So, several minutes interval are needed between SiH_4 injection and plasma ignition under standard discharge condition. To understand the effect of back diffusion of SiH_4, we apply a delayed SiH_4 gas injection condition[8] through adjusting the injected time t_{delay} before deposition starts. Different t_{delay} indicates different SiH_4 concentration at the time of plasma ignition. Figure 2 shows the Raman crystallinity of μc-Si:H films deposited directly on glass under different t_{delay} in the H_2 backgrounds. For comparison, crystallinity of μc-Si:H films deposited under standard discharge conditions is also shown in the figure. The abscissa in the figure represents the delayed time between silane injection and plasma ignition: '0s' means the plasma is ignited before silane injecting into the chamber; other points indicate that plasma is ignited after silane has injected into chamber for corresponding times. The Raman crystallinity of μc-Si:H films under delayed conditions are higher than that under standard discharge conditions, and the highest crystallinity is obtained at t_{delay} of 20 s for SC = 2 % and 30 s for SC = 4 %. In addition, under same t_{delay}, crystallinity decreases with the increase of SC.

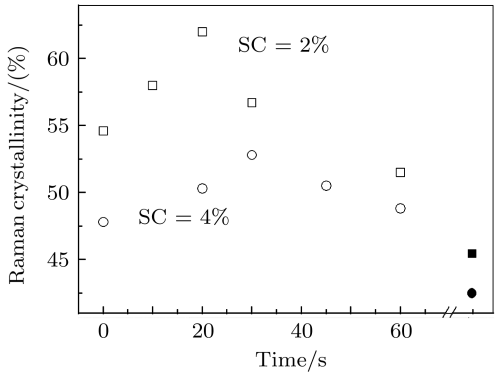


Fig. 2. Raman crystallinity of films deposited with different delay timescales under delayed conditions for different Silane concentrations: SC = 2% (open square); SC = 4% (open circle). The crystallinity of films deposited under standard discharge condition is also shown: SC = 2% (close square); SC = 4% (close circle).

Figure 3 shows the experimental measured spectra of the imaginary part, $< \varepsilon_2 >$, of the pseudo-dielectric function of μc-Si:H films deposited under different discharge conditions, and also the modeled curves. The obtained result presents the excellent agreement between the model and the experimental data on the whole spectral range. The schematic

view of the microstructural layers of the same films obtained from modeling of the SE data is presented in Table 1, where the fractional composition of constituent components and the layer thicknesses (d_l) are mentioned. The percentage volume fractions of crystalline, voids and amorphous content are denoted by F_c, F_v and F_a respectively. In this model diagram, we can see that under delayed discharge condition, F_c in bulk and surface layers are higher than that in the films deposited under standard conditions, and decrease with the increase of SiH_4 concentration. But, the F_v is high under delayed conditions. The thick incubation amorphous layer found under standard conditions is caused by the back diffusion of SiH_4 molecule from chamber. The SE and Raman analysis indicate that delayed SiH_4 density in the reactor is very effective in suppressing or removing the formation of the amorphous incubation layer in the initial μc-Si:H growth processing, and using this method we can deposit μc-Si:H films at relatively higher SiH_4 concentration.

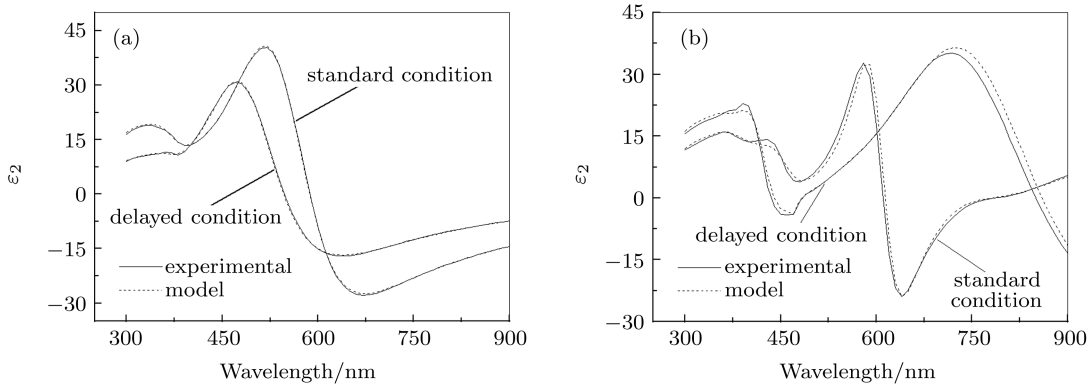


Fig. 3. Experimental (solid line) and model (dash line) imaginary part, $< \varepsilon_2 >$, of the pseudo-dielectric function of μc-Si:H films deposited under different discharge conditions at (a) SC = 2 %, t_{delay} = 20 s; (b) SC = 4 %, t_{delay} = 30 s.

Table 1. The schematic illustration of μc-Si:H films deposited under delayed and standard discharge conditions at SC = 2% and 4 %.

layers	conditions	2 %				4 %			
		d_l/nm	F_c/%	F_v/%	F_a/%	d_l/nm	F_c/%	F_v/%	F_a/%
interface layer	0 s	0				0.4			100
	10 s	0				–	–	–	–
	20 s	0				–	–	–	–
	30 s	0				0			
	standard	6.8			100	10.2			100
middle bulk layer	0 s	24.3	33.8	13.4	52.8	62.1	20.2	0	79.8
	10 s	34	40.3	7.8	51.9	–	–	–	–
	20 s	33.9	44.5	9.8	45.7	–	–	–	–
	30 s	25.9	40.9	6.6	52.5	33.5	28.1	0	71.9
	standard	25.4	25.4	0.2	74.4	102.2	5	0	95
surface layer	0 s	7.4	19	81	0	5.6	45.6	54.4	0
	10 s	9.4	30.2	69.8	0	–	–	–	–
	20 s	8.3	28.3	71.7	0	–	–	–	–
	30 s	10.7	14.8	85.2	0	7	22.7	77.3	0
	standard	5.7	9.2	45.7	45.1	9.3	16.7	48.9	34.4

3.2. Solar cells

In the μc-Si:H solar cells fabrication process, delayed conditions (SC = 4 %, t_{delay} = 30 s) is used during the deposition of the i-layer μc-Si:H film, and is also used for comparing standard discharge conditions. Figure 4 shows the Raman spectra of 100 nm μc-Si:H films deposited under different discharge conditions on 30 nm p-type μc-Si:H films. The calculated crystallinity of all films is higher than that deposited directly on bare glass

substrate, caused by the epitaxial growth, whereby the crystalline network of the p-type μc-Si:H film continued to propagate across the interface to the over-deposited film. Comparing with standard discharge conditions, we obtain the higher film crystallinity at p/i interface under delayed discharge conditions. These results correlate well with the assumed more amorphous growth conditions within the first minutes of deposition due to a back diffusion flux of SiH_4 under standard ignition conditions.

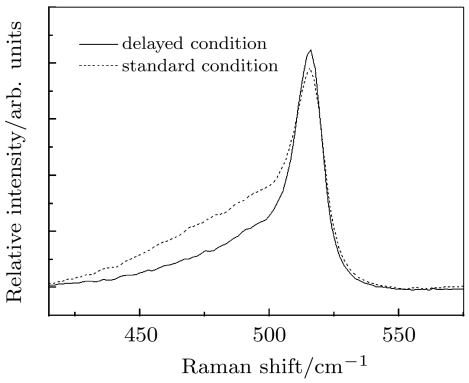


Fig. 4. Raman spectra of μc-Si:H films deposited under different discharge conditions on p-type μc-Si:H films.

Even under the same i-layer growth conditions, variation in the initial plasma ignition conditions could result in substantial changes in the properties of solar cell. Figure 5 shows the dependence of spectral response of the two μc-Si:H solar cells with i-layer deposited under different ignition conditions. Delayed initial SiH_4 density during i-layer deposition can improve spectral response in the middle and long wavelength region, hence increase the short circuit current density.

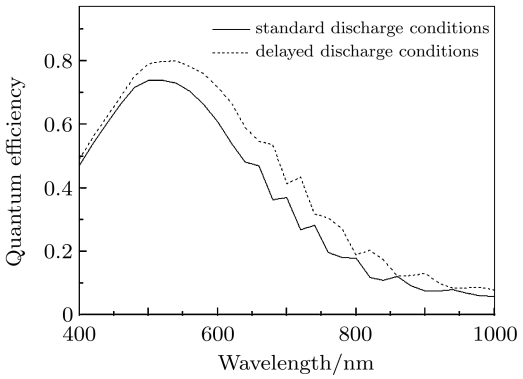


Fig. 5. Effect of different i-layers ignition conditions on the spectral response of single-junction p–i–n μc-Si:H solar cells.

3.3. Discussion

To explain our experiments, one modified zero-order analytical model is developed and is presented as follows.

Figure 6 shows the deposition process under standard discharge condition. Before plasma ignition the

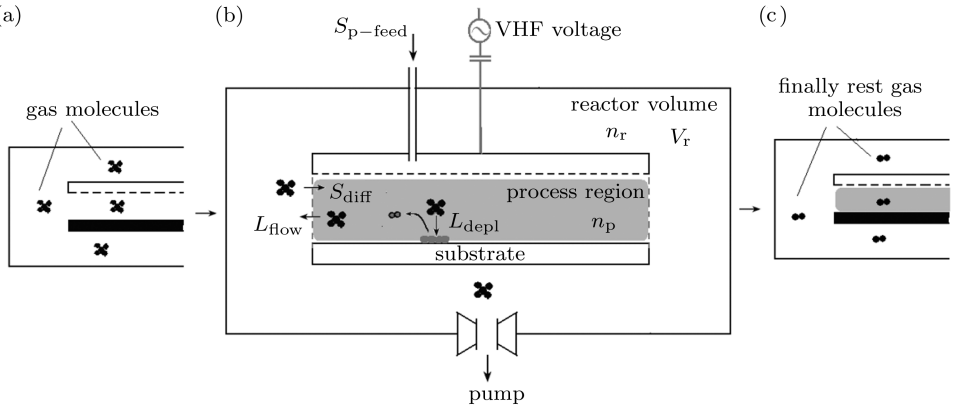


Fig. 6. Schematic representation of transient depletion in a cylindrical parallel plate plasma: (a) before processing; (b) initial deposition stage; (c) steady-state processing.

entire reactor is filled with the SiH_4/H_2 gas mixture and is characterized by an equilibrium initial source gas density

$$n_p(t=0) = n_r(t=0) = n_0, \tag{1}$$

where n_p, n_r, are the SiH_4 gas densities in the processing region and the reactor volume, respectively. This initial equilibrium source gas density n_0 is given by

$$n_0 = \frac{S_{\mathrm{p-feed}}}{Q}\frac{p}{k_{\mathrm{B}}T}, \tag{2}$$

where Q is the total flow in the reactor ([SiH_4]+[H_2]), p is the gas pressure, T is the gas temperature, $S_{\mathrm{p-feed}}$ is the feed gas rate and can be obtained directly by the SiH_4 gas flow towards the reactor volume, in which 1 sccm equals 4.5×10^{17} particles$\cdot$s^{-1}.

Once plasma is ignited, the source gas in this processing region is consumed and consequently depleted with the corresponding loss term given by L_{depl}. This leads to a density difference between processing region and reactor volume ($n_{\mathrm{p}} < n_{\mathrm{r}}$), the diffusive transport from reactor volume into processing region starts and slowly depletes the reactor volume of initially presented source gas. Since generally the reactor volume is much larger than the processing region, this slow reactor volume depletion has a higher impact on the materials processing than the fast initial local depletion. During this back diffusive transport phase, a quasi steady-state balance will establish itself in the processing region, in which the source gas diffusion into the processing region is quickly depleted. Mathematically,

$$L_{\mathrm{depl}} = S_{\mathrm{p-feed}} + S_{\mathrm{diff}} - L_{\mathrm{flow}}, \tag{3}$$

where S_{diff} and L_{flow} are the back and the directive flow between processing region and reactor volume, respectively.

In the microcrystalline silicon vapour phase deposition process, Eq. (3) is used to describe the deposition process in the process region. It starts at time $t = 0$ and is characterized by an instantaneous increase of L_{depl}.

The S_{diff} decreases with the deposition ($t \to \infty$), due to the decrease of n_{r} in the reactor. As S_{diff} gets a minimum, the steady-state deposition process is formed. The initial processing stage is defined as the time after processing has started but before a steady-state gas composition is reached. The steady-state is charactered by the steady-state depletion f_{depl}

$$f_{\mathrm{depl}} = 1 - \frac{n_{\mathrm{p}}(t\to\infty)}{n_0}. \tag{4}$$

The steady-state depletion f_{depl} can be calculated by the deposition rate r_{d}. Assuming uniform deposition on both electrodes, the steady-state depletion is given by

$$f_{\mathrm{depl}} = \frac{\pi R^2 r_{\mathrm{d}} n_{\mu\mathrm{c}}}{S_{\mathrm{p-feed}}}, \tag{5}$$

where $n_{\mu\mathrm{c}} =\sim 5\times10^{22}$ cm^{-3} is the Si atom density in the deposited silicon film.[10]

The reason for the occurrence of back diffusion is that the initial source gas density $n_{\mathrm{r}}(t=0) = n_{\mathrm{p}}(t=0) = n_0$ is higher than the steady-state source gas densities $n_{\mathrm{r}}(t\to\infty)$, $n_{\mathrm{p}}(t\to\infty)$. Thus, it should be possible to minimize the effect of back diffusion by realizing an initial source gas density close to the steady-state value.

The purpose of delayed initial source gas density is to realize $n_{\mathrm{r}}(t=0) \approx n_{\mathrm{r}}(t\to\infty)$ at a certain time t_{delay} before processing starts. For this initial value of $n_{\mathrm{r}}(t=-t_{\mathrm{delay}}) = 0$, and the optimized t_{delay} for $n_{\mathrm{r}}(t=0) = n_{\mathrm{r}}(t\to\infty)$ is given by

$$t_{\mathrm{delay}} = \tau_{\mathrm{r-res}} \ln\left(\frac{1}{1-n_{\mathrm{r}}(t\to\infty)/n_0}\right), \tag{6}$$

in which $\tau_{\mathrm{r-res}}$ is the gas residence time in the reactor and is defined as

$$\tau_{\mathrm{r-res}} = \frac{n_0 V_{\mathrm{r}}}{S_{\mathrm{p-feed}}}, \tag{7}$$

where V_{r} is the reactor volume.

Equation (6) describes how the initial source gas density in the reactor volume $n_{\mathrm{r}}(t=0)$ can be varied between $0 < n_{\mathrm{r}}(t=0) < n_0$ by tuning t_{delay}. In the steady-state deposition process, $n_{\mathrm{r}}(t\to\infty) = n_{\mathrm{p}}(t\to\infty)$. So, Eq. (6) changes to

$$t_{\mathrm{delay}} = \tau_{\mathrm{r-res}} \ln\left(\frac{1}{1-n_{\mathrm{p}}(t\to\infty)/n_0}\right). \tag{8}$$

In this modified model, the only one important parameter needs to be confirmed is the deposition rate r_{d}, which can be measured easily through experiment. In our experiment, r_{d} equals 0.38 nm/s for SC = 2 % and 0.64 nm/s for SC = 4 %,[11] respectively. Using the analytical expressions derived above to describe the back diffusion under the experimental conditions discussed in Section 2, we show the results in Table 2. Under our experimental conditions, the steady-state depletion f_{depl} is 60 % for SC = 2 % and 50 % for SC = 4 %, due to the lower deposition pressure. The modeled t_{delay} equals 22 s for SC = 2 % and 30 s for SC = 4 %, it is in good agreement with experiments.

Table 2. Input and output quantities of the model applied to the conditions of Section 2.

input quantity	symbol	value		unit	
reactor volume	$V_{\rm r}$	1.1×10^5		$\rm cm^3$	
electrode radius	R	15		cm	
electrode gap	D	1.5		m	
SiH_4 flow (showerhead)	$S_{\rm p-feed}$	5	10	sccm	
total flow	Q	250		sccm	
pressure	p	3×10^2		Pa	
temperature	T	5×10^2		K	
deposition rate	$r_{\rm d}$	0.38	0.64	nm/s	
output quantity	symbol	value		unit	equation
equilibrium SiH_4 density	n_0	8.7×10^{14}	1.7×10^{15}	$\rm cm^{-3}$	(2)
residence time in reactor volume	$\tau_{\rm r-res}$	43		s	(7)
steady-state SiH_4 depletion	$f_{\rm depl}$	60	50	%	(5)
steady-state SiH_4 concentration	$n_{\rm p}(t\rightarrow\infty)$	3.5×10^{14}	8.5×10^{15}	$\rm cm^{-3}$	(4)
optimized delayed time	$t_{\rm delay}$	22	30	s	(6)

4. Conclusions

The back diffusion of SiH_4 molecules affects the initial stage of materials processing, such as crystallite nucleation and microstructure properties. The occurrence of SiH_4 back diffusion could be prevented by using delayed initial SiH_4 density in the reactor, in which the SiH_4 flow is switched on only shortly before plasma ignition. Combining this method with solar cell fabrication, we obtain a high spectral response in the middle and long wavelength region. The modified zero-order analytical model is developed, and the optimized delayed time can be deduced quickly and exactly by the one important parameter $r_{\rm d}$.

References

[1] van den Donker M N, Rech B, Finger F, Kessels W M M and van de Sanden M C M 2005 *Appl. Phys. Lett.* **87** 263503

[2] Losurdo M, Giangregorio M, Sacchetti A, Capezzuto P, Bruno G and Giorgis F 2006 *Appl. Surf. Sci.* **253** 287

[3] Sorokin M, Kroesen G M W and Stoffels W W 2004 *IEEE Trans. Plasma Sci.* **32** 731

[4] Roschek T, Rech B, Müller J, Schmitz R and Wagner H 2004 *Thin Solid Films* **451–452** 466

[5] Guo L, Kondo M, Fukawa M, Saitoh K and Matsuda A 1998 *Jpn. J. Appl. Phys.* Part 2 **37** L1116

[6] Rech B, Roschek T, Repmann T, Müller J, Schmitz R and Appenzeller W 2003 *Thin Solid Films* **427** 157

[7] Amanitides E, Hammad A, Katsia E and Mataras D 2005 *J. Appl. Phys.* **97** 073303

[8] van den Donker M N, Rech B, Kessels W M M and van de Sanden M C M 2007 *New Journal of Physics* **9** 280

[9] Chen Y S, Gao X Y, Yang S E, Lu J X and Gu J H 2007 *Acta Phys. Sin.* **56** 4122 (in Chinese)

[10] Custer J S, Thompson M O, Jacobson D C, Poate J M, Roorda S, Sinke W C and Spaepen F 1993 *Appl. Phys. Lett.* **64** 437

[11] Chen Y S, Wang J H, Lu J X, Zheng W, Gu J H, Yang S E, Gao X Y, Guo X J, Zhao S L and Gao Z 2008 *Chin. Phys.* B **17** 3464